Strong mechanical squeezing and optomechanical steering via continuous monitoring in optomechanical systems

Huatang Tan[*] and Huiping Zhan[†]

Department of Physics, Huazhong Normal University, Wuhan 430079, China

In this paper, we first consider the generation of mechanical squeezing in a dispersively or dissipatively coupled optomechanical system by continuously homodyning the output field of the optomechanical cavity. It is found that strong steady-state mechanical squeezing beyond the 3 dB limit can be achieved in both of the optomechanical systems. The properties of the squeezing are quite different for the two types of systems and the reasons for the differences are analyzed. We next consider the achievement of optomechanical steering in the dispersive or dissipative optomechanical system via continuously monitoring the position of the mechanical oscillator. It is revealed that the monitoring can lead the steady-state optomechanical entanglement to be enhanced considerably such that strong steerable correlations can be achieved between the mechanical oscillator and the cavity field. The effects of thermal phonons are studied and it is shown that the generated squeezing and steering are quite robust against the thermal fluctuations.

I. INTRODUCTION

The generation of squeezed states of a macroscopic mechanical resonator has always attracted a lot of attention due to its usefulness for, e.g., demonstrating macroscopic quantum effects, ultraprecision measurements [1], and quantum informatics of continuous variables [2]. Generically, in analogy to the squeezed-light generation in quantum optics, one can use a mechanical parametric downconvertor (via, e.g., modulating mechanical spring at twice the mechanical resonance) to achieve mechanical squeezed states [3,4]. However, the squeezing in the steady-state regime via this process is limited by the so-called 3 dB limit (i.e., the maximal squeezing in the steady-state regime is about fifty percent of vacuum fluctuations). To surpass the limit, a variety of schemes has been put forward recently. These include injecting broadband squeezed light into an optomechanical system [5], constructing a detuned mechanical parametric downconvertor which is subject to weak time-continuous measurements [6], putting an optical parametric downconvertor inside an optomechanical cavity combined with quantum feedback [7,8], exploring strong mechanical nonlinearity [9], and applying two-color driving on an optomechanical cavity and quantum reservoir engineering [10,11], which has been experimentally realized [12].

Quantum steering, originally termed by Schrödinger in his response to the well-known Einstein-Podolsky-Rosen (EPR) paradox [13,14], characterizes the ability to nonlocally steer quantum states of a particle entangled with another remote particle via local measurements. It is an intrinsic quantum nonlocality, distinct from Bell nonlocality (the violation of Bell inequality) [15,16], as shown recently by Wiseman *et al.* and Jones *et al.* in Refs. [17,18]. They verified that the states exhibiting Bell nonlocality are a subset of steerable states which are, in turn, a subset of entangled (inseparable) states, i.e., steering is intermediate between entanglement and Bell nonlocality. Distinct from entanglement and Bell nonlocality, steering is intrinsically asymmetric with respect to the two particles and thus directional. There may exist one-way steering which allows us to steer the states of one particle by measuring the other, but not vice versa [19–24]. Besides being of fundamental interest, EPR steering also has potential applications, e.g., one-sided device-independent quantum cryptography [25,26], subchannel discrimination [27], and secure quantum teleportation [28]. Additionally, by utilizing steerable correlations, desirable quantum states can be achieved via local measurements [29–32]. Nowadays, quantum steering has been experimentally realized in a variety of systems [21–24,33–40].

Over the past decade, quantum optomechanics, which involves the hybrid coupling between a mechanical resonator and an electromagnetic field, has emerged as a new research field [41]. Optomechanical systems hold great potential to test quantum physics on a macroscopic scale, apart from possible applications in, e.g., quantum information processing [42–46] and ultrahigh-precision measurements [47–49]. Recent experiments have achieved a few of the quantum effects in optomechanical systems, such as optical and mechanical squeezed states [50–52], light-mechanical entangled states of continuous and discrete variables [53,54], Gaussian entanglement between two mechanical resonators [55], nonclassical correlations between single photons and phonons from a mechanical oscillator [56], heralded single-phonon Fock states of a mechanical oscillator [57], and optomechanical Bell nonlocality involving a macroscopic massive mechanical resonator [58]. Theoretically, the scheme for achieving optomechanical

---

[*]tht@mail.ccnu.edu.cn

[†]1085879676@qq.com

023843-1

Bell nonlocality of Gaussian states has also been proposed [59].

In this paper, we consider the generation of strong mechanical squeezing and optomechanical steering—anther kind of quantum nonlocality—in the regime of steady states, respectively, by continuously monitoring the cavity field and the position of the mechanical oscillator in dispersively or dissipatively coupled optomechanical systems. We note that quantum control of optomechanical systems via continuous measurements to realize, e.g., ground-state cooling and non-classical mechanical states has been investigated [6,60–65]. Meanwhile, the control of the mechanical oscillators via individual measurements in pulsed optomechanics has also been investigated [66–68]. We first consider the generation of mechanical squeezing in a dispersively or dissipatively coupled optomechanical system by continuously homodyning the output of the cavity field. It is found that strong steady-state mechanical squeezing beyond the 3 dB limit can be achieved for the two types of coupling, but the properties of the mechanical squeezing are quite different. The reasons for the differences are analyzed. We next consider the achievement of steady-state optomechanical steering in the optomechanical systems via continuously monitoring the position of the mechanical oscillator. It is revealed that the monitoring of the mechanical position can lead the steady-state optomechanical entanglement to be considerably enhanced such that strong steerable correlations can be achieved between the mechanical oscillator and the cavity field in both of the coupled systems. We also study the effects of thermal phonons and it is shown that the generated squeezing and steering are robust against the thermal fluctuations.

The remainder of this paper is organized as follows. In Sec. II, the system is introduced and the working equations are presented. In Sec. III, the properties of the mechanical squeezing and optomechanical steering in a dispersive or dissipative optomechanical system under time-continuous measurements are investigated in detail. In Sec. IV, we give the main summary.

II. SYSTEM AND EQUATIONS

A. System

As schematically shown in Fig. 1(a), we consider a generic optomechanical system in which a mechanical resonator (described by the operator $\hat{b}_m$) of frequency ω_m is dispersively or dissipatively coupled to a laser-driven cavity field (denoted by the operator $\hat{a}_c$). This means that the cavity resonance $\tilde{\omega}_c$ or the dissipation rate $\tilde{\kappa}_c$ is modulated by the position $\hat{X}_m$ of the mechanical oscillator, leading to dispersive or dissipative optomechanical coupling, respectively. To achieve mechanical squeezing, the cavity output is subject to time-continuous homodyne detection. As depicted in Fig. 1(b), we also consider the establishment of optomechanical steering between the cavity field $\hat{a}_c$ and the mechanical oscillator $\hat{b}_m$ by continuous monitoring of the position of the mechanical oscillator. To this end, we consider the coupling of the mechanical oscillator to anther cavity of resonance $\tilde{\omega}_t$. The cavity field is called the transducer field and denoted by the operator $\hat{a}_t$. This two-cavity optomechanical system can be realized with two microwave cavities mediated by a mechanical oscillator
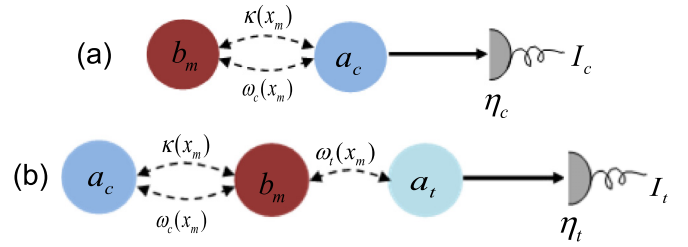

FIG. 1. (a) Generating strong mechanical squeezing in a dispersive or dissipative optomechanical system (a_c, b_m) by continuously homodyning the output field of the cavity. (b) Achieving strong optomechanical steerable correlations in a dispersive or dissipative optomechanical system (a_c, b_m) by continuously monitoring the position X_m of the mechanical oscillator. The position monitoring can be realized by dispersively coupling the mechanical oscillator weakly to a bad cavity a_t whose output field is subject to continuous homodyne detection. The parameters I_j and η_j ($j = c, t$) denote the detection currents and efficiencies, respectively.

[69,70] or optoelectromechanical systems composed of a microwave and optical cavities sharing a mechanical resonator [71]. We will later show that in the bad cavity limit, the homodyne detection of the transducer field can approximately give the mechanical position. In the rotating frame, with respect to the driving frequencies ω_{dj} ($j = s, t$) of the two cavities, the effective Hamiltonian of the system ($\hbar = 1$) can be written as

$$\hat{H} = \sum_{j=c,t}[\tilde{\omega}_j(\hat{X}_m) - \omega_{dj}]\hat{a}_j^\dagger\hat{a}_j + \omega_m\hat{b}_m^\dagger\hat{b}_m$$
$$+ i\sqrt{\tilde{\kappa}_c(\hat{X}_m)}\left(\hat{a}_c^{\text{in}\dagger}\hat{a}_c - \hat{a}_c^\dagger\hat{a}_c^{\text{in}}\right)$$
$$+ i\sqrt{\kappa_t}\left(\hat{a}_t^{\text{in}\dagger}\hat{a}_t - \hat{a}_t^\dagger\hat{a}_t^{\text{in}}\right), \tag{1}$$

where $\hat{X}_m \equiv \frac{1}{\sqrt{2}}(\hat{b}_m + \hat{b}_m^\dagger)$ is the dimensionless displacement operator of the mechanical oscillator, $\hat{a}_j^{\text{in}}$ denote the cavity input fields consisting of coherent driving and vacuum noise components, and κ_t is the dissipation rate of the transducer cavity.

By taking into account the damping of the mechanical oscillator, the Langevin equations of motion for the operators $\hat{a}_j$ and $\hat{b}_m$ are found to be

$$\frac{d}{dt}\hat{a}_c = -\left\{\frac{\tilde{\kappa}_c(\hat{X}_m)}{2} + i[\tilde{\omega}_c(\hat{X}_m) - \omega_{dc}]\right\}\hat{a}_c - \sqrt{\tilde{\kappa}_c(\hat{X}_m)}\hat{a}_c^{\text{in}}(t),$$
$$\tag{2a}$$

$$\frac{d}{dt}\hat{a}_t = -\left\{\frac{\kappa_t}{2} + i[\tilde{\omega}_t(\hat{X}_m) - \omega_{dt}]\right\}\hat{a}_t - \sqrt{\kappa_t}\hat{a}_t^{\text{in}}(t), \tag{2b}$$

$$\frac{d}{dt}\hat{b}_m = -\left[\frac{\gamma_m}{2} + i\omega_m\right]\hat{b}_m + i\sum_j[\tilde{\omega}_j(\hat{X}_m), \hat{b}_m]\hat{a}_j^\dagger\hat{a}_j$$
$$- [\sqrt{\tilde{\kappa}_c(\hat{X}_m)}, \hat{b}_m]\left(\hat{a}_c^{\text{in}\dagger}\hat{a}_c - \hat{a}_c^\dagger\hat{a}_c^{\text{in}}\right) - \sqrt{\gamma_m}\hat{b}_{\text{in}}(t), \tag{2c}$$

where γ_m denotes the mechanical damping rate and the mechanical noise operator $\hat{b}_{\text{in}}(t)$ has the nonzero correlations $\langle\hat{b}_{\text{in}}(t)\hat{b}_{\text{in}}^\dagger(t')\rangle = (\bar{n}_{th} + 1)\delta(t - t')$ and $\langle\hat{b}_{\text{in}}^\dagger(t)\hat{b}_{\text{in}}(t')\rangle = \bar{n}_{th}\delta(t - t')$, with $\bar{n}_{th} \equiv (e^{\hbar\omega_m/k_BT} - 1)^{-1}$ denoting the mean number of thermal phonons of the thermal environment of the

mechanical oscillator at temperature T, with k_B the Boltzmann constant.

We consider the situation that the position-dependent frequencies $\tilde{\omega}_j(\hat{X}_m)$ and linewidth $\tilde{\kappa}_c(\hat{X}_m)$ are expanded to the first order in the position operator $\hat{X}_m$, i.e., $\tilde{\omega}_j(\hat{X}_m) \simeq \omega_j - \sqrt{2}g_{j\omega}\hat{X}_m$ and $\tilde{\kappa}_c(\hat{X}_m) \simeq \kappa_c + \sqrt{2}g_{c\kappa}\hat{X}_m$, where the dispersive and dissipative couplings are $g_{j\omega} = -\frac{\partial\tilde{\omega}_j}{\sqrt{2}\partial X_m}$ and $g_{c\kappa} = \frac{\partial\tilde{\kappa}_c}{\sqrt{2}\partial X_m}$, respectively. We then have $\sqrt{\tilde{\kappa}_c(\hat{X}_m)} \simeq \sqrt{\kappa_c}(1 + \frac{g_{c\kappa}\hat{X}_m}{\sqrt{2}\kappa_c})$. In this way, the Langevin equations of Eq. (2) reduce to

$$\frac{d}{dt}\hat{a}_c = -\left[\frac{\kappa_c}{2}\left(1 + \frac{\sqrt{2}g_{c\kappa}}{\kappa_c}\hat{X}_m\right) + i\delta_c - i\sqrt{2}g_{c\omega}\hat{X}_m\right]\hat{a}_c$$
$$- \sqrt{\kappa_c}\left(1 + \frac{g_{c\kappa}}{\sqrt{2}\kappa_c}\hat{X}_m\right)\hat{a}_c^{\text{in}}(t), \tag{3a}$$

$$\frac{d}{dt}\hat{a}_t = -\left[\frac{\kappa_t}{2} + i\delta_t - i\sqrt{2}g_{t\omega}\hat{X}_m\right]\hat{a}_t - \sqrt{\kappa_t}\hat{a}_t^{\text{in}}(t), \tag{3b}$$

$$\frac{d}{dt}\hat{b}_m = -\left[\frac{\gamma_m}{2} + i\omega_m\right]\hat{b}_m + i\sum_j g_{j\omega}\hat{a}_j^\dagger\hat{a}_j \tag{3c}$$

$$+ \frac{g_{c\kappa}}{2\sqrt{\kappa_c}}\left(\hat{a}_c^{\text{in}\dagger}\hat{a}_c - \hat{a}_c^\dagger\hat{a}_c^{\text{in}}\right) - \sqrt{\gamma_m}\hat{b}_{\text{in}}(t), \tag{3d}$$

where the detuning $\delta_j = \omega_j - \omega_{dj}$.

The above nonlinear equations of Eq. (3) can be linearized around the steady-state amplitudes of the operators $\hat{a}_j$, $\hat{b}_m$, and $\hat{a}_j^{\text{in}}$ as $\hat{a}_j = \bar{a}_j^{ss} + \delta\hat{a}_j$, $\hat{b}_m = \bar{b}_m^{ss} + \delta\hat{b}_m$, and $\hat{a}_j^{\text{in}} = \bar{a}_j^{\text{in,ss}} + \delta\hat{a}_j^{\text{in}}$ when $|\bar{\mathcal{O}}^{ss}|^2 \gg \langle\delta\hat{\mathcal{O}}\delta\hat{\mathcal{O}}^\dagger\rangle$ for operator $\hat{\mathcal{O}} = \{\hat{a}_j, \hat{b}_m\}$. Here the steady-state amplitudes $\bar{a}_j^{ss} \approx -\frac{2\sqrt{\kappa_c}\bar{a}_j^{\text{in,ss}}}{\kappa_j + 2i\Delta_j}$, with the detuning $\Delta_j = \delta_j - \sqrt{2}g_{j\omega}\text{Re}[\bar{X}_m^{ss}]$, and $\bar{b}_m^{ss} \approx \frac{\sum_j g_{j\omega}|\bar{a}_j^{ss}|^2 + g_{c\kappa}\text{Im}[\bar{a}_j^{\text{in,ss}*}\bar{a}_j^{ss}]/2\sqrt{\kappa_c}}{\omega_m}$. The operators $\delta\hat{a}_j$ and $\delta\hat{b}_m$ describe the quantum fluctuations of the cavity and mechanical modes, and $\delta\hat{a}_j^{\text{in}}$ describe the vacuum inputs of the cavities. In the following, the script δ is omitted for simplicity. Then, the linearized Langevin equations can be derived as (see the Appendix)

$$\frac{d}{dt}\hat{a}_c = -\left(\frac{\kappa_c}{2} + i\Delta_c\right)\hat{a}_c - \left[\frac{G_\kappa}{4} - i\left(G_\omega + \frac{G_\kappa\Delta_c}{2\kappa_c}\right)\right]$$
$$\times (\hat{b}_m + \hat{b}_m^\dagger) - \sqrt{\kappa_c}\hat{a}_c^{\text{in}}(t), \tag{4a}$$

$$\frac{d}{dt}\hat{a}_t = -\left(\frac{\kappa_t}{2} + i\Delta_t\right)\hat{a}_t + iG_t(\hat{b}_m + \hat{b}_m^\dagger) - \sqrt{\kappa_t}\hat{a}_t^{\text{in}}(t), \tag{4b}$$

$$\frac{d}{dt}\hat{b}_m = -\left[\frac{\gamma_m}{2} + i\omega_m\right]\hat{b}_m - \left[\frac{G_\kappa}{4} - i\left(G_\omega + \frac{G_\kappa\Delta_c}{2\kappa_c}\right)\right]\hat{a}_c$$
$$+ \left[\frac{G_\kappa}{4} + i\left(G_\omega + \frac{G_\kappa\Delta_c}{2\kappa_c}\right)\right]\hat{a}_c^\dagger + iG_t(\hat{a}_c + \hat{a}_c^\dagger)$$
$$- \frac{G_k}{2\sqrt{\kappa_c}}\hat{a}_c^{\text{in}}(t) + \frac{G_\kappa}{2\sqrt{\kappa_c}}\hat{a}_c^{\text{in}\dagger}(t) - \sqrt{\gamma_m}\hat{b}_{\text{in}}(t), \tag{4c}$$

where $G_\omega = g_{c\omega}\bar{a}_c^{ss}$, $G_t = g_{t\omega}\bar{a}_t^{ss}$, and $G_\kappa = g_{c\kappa}\bar{a}_c^{ss}$ are, respectively, the enhanced dispersive and dissipative optomechanical coupling strengths.

From Eq. (4), the effective linearized Hamiltonian can be found to be

$$\hat{H}_{\text{eff}} = \sum_j \Delta_j\hat{a}_j^\dagger\hat{a}_j + \omega_m\hat{b}_m^\dagger\hat{b}_m - G_t(\hat{a}_t + \hat{a}_t^\dagger)(\hat{b}_m + \hat{b}_m^\dagger)$$
$$- \left(G_\omega + \frac{\Delta_c}{2\kappa_c}G_\kappa\right)(\hat{a}_c + \hat{a}_c^\dagger)(\hat{b}_m + \hat{b}_m^\dagger), \tag{5}$$

which shows that the dissipative coupling can also lead to the same optomechanical interaction (the terms related to G_κ) as the dispersive coupling, but it disappears for resonant driving $\Delta_c = 0$. From Eq. (4), we see that the cavity field $\hat{a}_c$ and the mechanical oscillator are simultaneously coupled to a common vacuum reservoir (denoted by $\hat{a}_c^{\text{in}}$), giving rise to the dissipative coupling between the mechanical oscillator and the cavity field. This can be explicitly seen from the master equation for the density operator $\hat{\rho}$ of the whole system, which is equivalent to the Langevin equation of Eq. (4) and given by

$$\frac{d}{dt}\hat{\rho} = -i[\hat{H}_{\text{eff}}, \hat{\rho}] + \sum_j \kappa_j\mathcal{L}[\hat{a}_j]\hat{\rho}$$
$$+ \gamma_m(\bar{n}_{th} + 1)\mathcal{L}[\hat{b}_m]\hat{\rho} + \gamma_m\bar{n}_{th}\mathcal{L}[\hat{b}_m^\dagger]\hat{\rho}$$
$$+ \frac{G_\kappa^2}{8\kappa_c}\mathcal{L}[\hat{b}_m + \hat{b}_m^\dagger]\hat{\rho} + \frac{G_\kappa}{4}[2\hat{a}_s\hat{\rho}(\hat{b}_m + \hat{b}_m^\dagger)$$
$$- (\hat{b}_m + \hat{b}_m^\dagger)\hat{a}_s\hat{\rho} - \hat{\rho}(\hat{b}_m + \hat{b}_m^\dagger)\hat{a}_s + \text{H.c.}], \tag{6}$$

where $\mathcal{L}[\hat{o}]\hat{\rho} = \hat{o}\hat{\rho}\hat{o}^\dagger - \frac{1}{2}(\hat{o}^\dagger\hat{o}\hat{\rho} + \hat{\rho}\hat{o}^\dagger\hat{o})$. Different from purely dispersive optomechanical coupling, purely dissipative optomechanical coupling can lead to phonon heating (the first term in the third line) and dissipative optomechanical coupling (the terms related to G_κ in the third and last lines).

B. Under time-continuous measurements

We consider that the outputs of the cavity field $\hat{a}_c$ and the transducer field $\hat{a}_t$ are subject to time-continuous homodyne detection. For the cavity outputs

$$\hat{a}_c^{\text{out}}(t) = \sqrt{\kappa_c}\hat{a}_c + \frac{G_\kappa}{\sqrt{2}\kappa_c}\hat{X}_m + \hat{a}_c^{\text{in}}(t), \tag{7a}$$

$$\hat{a}_t^{\text{out}}(t) = \sqrt{\kappa_t}\hat{a}_t + \hat{a}_t^{\text{in}}(t), \tag{7b}$$

the generalized quadratures $\hat{X}_j^{\phi_j} = \frac{1}{\sqrt{2}}(\hat{\mathcal{O}}_j^{\text{out}}e^{i\phi_j} + \hat{\mathcal{O}}_j^{\text{out}\dagger}e^{-i\phi_j})$ are subject to homodyne detection, where the phases ϕ_j are controllable via adjusting the local fields in the detection. The corresponding detection currents are

$$I_c^{\phi_c}dt = \sqrt{\eta_c\kappa_c}\langle\hat{a}_c e^{i\phi_c} + \hat{a}_c^\dagger e^{-i\phi_c}\rangle dt$$
$$+ \frac{\sqrt{2\eta_c}G_\kappa\cos\phi_c}{\sqrt{\kappa_c}}\hat{X}_m dt + dW_s, \tag{8a}$$

$$I_t^{\phi_t}dt = \sqrt{\eta_t\kappa_t}\langle\hat{a}_t e^{i\phi_t} + \hat{a}_t^\dagger e^{-i\phi_t}\rangle dt + dW_t, \tag{8b}$$

where η_j are the detection efficiencies and dW_j are the Wiener increments satisfying $dW_j dW_{j'} = dt\delta_{jj'}$. From the above equations, we see that for the dissipative coupling, the detection current $I_c^{\phi_c}$ explicitly depends on the position $\hat{X}_m$ of the mechanical oscillator, different from the current $I_t^{\phi_t}$ for dispersive coupling. This is because the motion of the mechanical oscillator is directly coupled to the input field $\hat{a}_c^{\text{in}}(t)$ in dissipatively coupled optomechanical systems and

therefore monitoring the environment (output field) of the cavity field $\hat{a}_c$ is mechanically dependent.

Depending on the detection results, the stochastic master equation for the unnormalized conditional state $\hat{\bar{\rho}}_c$ is given by [72]

$$
\begin{aligned}
d\hat{\bar{\rho}}_c = &-i[\hat{H}_{\text{eff}}, \hat{\bar{\rho}}_c]dt + \sum_j \kappa_j \mathcal{L}[\hat{a}_j]\hat{\rho}_c dt \\
&+ \gamma_m(\bar{n}_{th}+1)\mathcal{L}[\hat{b}_m]\hat{\bar{\rho}}_c dt + \gamma_m \bar{n}_{th}\mathcal{L}[\hat{b}_m^\dagger]\hat{\bar{\rho}}_c dt \\
&+ \frac{G_\kappa^2}{8\kappa_c}\mathcal{L}[\hat{b}_m+\hat{b}_m^\dagger]\hat{\bar{\rho}}_c dt + \frac{G_\kappa}{4}[2\hat{a}_c\hat{\bar{\rho}}_c(\hat{b}_m+\hat{b}_m^\dagger) \\
&- (\hat{b}_m+\hat{b}_m^\dagger)\hat{a}_c\hat{\bar{\rho}}_c - \hat{\bar{\rho}}_c(\hat{b}_m+\hat{b}_m^\dagger)\hat{a}_c + \text{H.c.}]dt \\
&+ \left[\left(\sqrt{\eta_c\kappa_c}\hat{a}_c + \frac{\sqrt{\eta_s}G_\kappa}{\sqrt{2}\kappa_c}\hat{X}_m\right)e^{i\phi_c}\hat{\bar{\rho}}_c + \text{H.c.}\right]I_c^{\phi_c}dt \\
&+ \sqrt{\eta_t\kappa_t}(\hat{a}_t e^{i\phi_t}\hat{\bar{\rho}}_c + \text{H.c.})I_t^{\phi_t}dt,
\end{aligned}
\tag{9}
$$

where the parameters η_j account for the detection efficiencies. The master equation for the normalized state $\hat{\rho}_c$ can be found to be

$$
\begin{aligned}
d\hat{\rho}_c = &-i[\hat{H}_{\text{eff}}, \hat{\rho}_c]dt + \sum_j \kappa_j \mathcal{L}[\hat{a}_j]\hat{\rho}_c dt \\
&+ \gamma_m(\bar{n}_{th}+1)\mathcal{L}[\hat{b}_m]\hat{\rho}_c dt + \gamma_m \bar{n}_{th}\mathcal{L}[\hat{b}_m^\dagger]\hat{\rho}_c dt \\
&+ \frac{G_\kappa^2}{8\kappa_s}\mathcal{L}[\hat{b}_m+\hat{b}_m^\dagger]\hat{\rho}_c dt + \frac{G_\kappa}{4}[2\hat{a}_s\hat{\rho}_c(\hat{b}_m+\hat{b}_m^\dagger) \\
&- (\hat{b}_m+\hat{b}_m^\dagger)\hat{a}_c\hat{\rho}_c - \hat{\rho}_c(\hat{b}_m+\hat{b}_m^\dagger)\hat{a}_c + \text{H.c.}]dt \\
&+ \mathcal{H}\left[\left(\sqrt{\eta_c\kappa_c}\hat{a}_s + \frac{\sqrt{\eta_c}G_\kappa}{\sqrt{2}\kappa_c}\hat{X}_m\right)e^{i\phi_c}\right]\hat{\rho}_c dW_c \\
&+ \sqrt{\eta_t\kappa_t}\mathcal{H}[\hat{a}_t e^{i\phi_t}]\hat{\rho}_c dW_t,
\end{aligned}
\tag{10}
$$

where the nonlinear terms $\mathcal{H}[\hat{\mathcal{O}}]\hat{\rho} = (\hat{\mathcal{O}}-\langle\hat{\mathcal{O}}\rangle)\hat{\rho} + \hat{\rho}(\hat{\mathcal{O}}-\langle\hat{\mathcal{O}}\rangle)$, describing the nonlinear effects due to the time-continuous measurements.

We further assume that the dynamics of the transducer cavity field $\hat{a}_t$ is much faster on the timescale than the dynamics of the mechanical system on the condition $\kappa_t \gg \{G_t, \omega_m, \bar{n}_{th}\gamma_m\}$. That is to say, the minimum time required for achieving steady states for the transducer field is much shorter than that for the mechanical system, and thus the transducer field can be adiabatically eliminated. In this way, we have $\hat{a}_t \approx -\frac{2iG_t}{\kappa_t}(\hat{b}_m+\hat{b}_m^\dagger) + \frac{2}{\sqrt{\kappa_t}}\hat{a}_t^{\text{in}}(t)$, when $\kappa_t \gg \Delta_t \sim \omega_m$. Therefore, we can see that the measurement of the quadratures of the output field $\hat{a}_t^{\text{out}}$ can allow us to infer the position of the mechanical oscillator, merely introducing extra vacuum fluctuations. The conditional master equation for the density matrix $\hat{\bar{\rho}}_c$ of the subsystem of the cavity field $\hat{a}_c$ and the mechanical oscillator after the adiabatical elimination can be found to be

$$
\begin{aligned}
d\hat{\bar{\rho}}_c = &-i[\hat{\bar{H}}_{\text{eff}}, \hat{\bar{\rho}}_c]dt + \kappa_c \mathcal{L}[\hat{a}_c]\hat{\bar{\rho}}_c dt + \Gamma_m \mathcal{L}[\hat{X}_m]\hat{\bar{\rho}}_c dt \\
&+ \gamma_m(\bar{n}_{th}+1)\mathcal{L}[\hat{b}_m]\hat{\bar{\rho}}_c dt + \gamma_m \bar{n}_{th}\mathcal{L}[\hat{b}_m^\dagger]\hat{\bar{\rho}}_c dt \\
&+ \mathcal{H}\left[\left(\sqrt{\eta_c\kappa_c}\hat{a}_c + \frac{\sqrt{\eta_c}G_\kappa}{\sqrt{2}\kappa_c}\hat{X}_m\right)e^{i\phi_c}\right]\hat{\bar{\rho}}_c dW_c \\
&+ \sqrt{\eta_t\Gamma_m}\mathcal{H}[\hat{X}_m]\hat{\bar{\rho}}_c dW_t,
\end{aligned}
\tag{11}
$$

where we have chosen the phase $\phi_t = \frac{\pi}{2}$ by adjusting the local field, the Hamiltonian

$$
\begin{aligned}
\hat{H}_{\text{eff}} \approx &\Delta_c \hat{a}_c^\dagger \hat{a}_c + \omega_m \hat{b}_m^\dagger \hat{b}_m \\
&- \left(G_\omega + \frac{\Delta_c}{2\kappa_c}G_\kappa\right)(\hat{a}_c+\hat{a}_c^\dagger)(\hat{b}_m+\hat{b}_m^\dagger),
\end{aligned}
\tag{12}
$$

and $\Gamma_m = \frac{8G_t^2}{\kappa_t}$. From the above equation, we see that the weak coupling of the mechanical oscillator to the overdamped transducer field brings about a decohering environment to the mechanical oscillator (the third term), while the last term describes the direct measurement of the position of the mechanical oscillator which results from the continuous monitoring of the effective mechanical environment.

C. Correlation matrix

The above master equation of Eq. (11) determines the properties of the dispersively or dissipatively optomechanical system subject to continuous monitoring of the cavity output or the position of the mechanical oscillator. When the system starts from a Gaussian state, it remains Gaussian and its properties are determined by the correlation matrix σ, defined as $\sigma_{ii'} = \langle\mu_i\mu_{i'} + \mu_{i'}\mu_i\rangle/2 - \langle\mu_i\rangle\langle\mu_{i'}\rangle$, with $\mu = (\hat{X}_c, \hat{Y}_c, \hat{X}_m, \hat{Y}_m)$, where $\hat{X}_c$ and $\hat{Y}_c$ are the quadrature operators of the cavity field $\hat{a}_c$. From Eq. (11), the first moments $\bar{\mu} \equiv \langle\mu^T\rangle$ and the covariance matrix σ are determined by

$$
\frac{d}{dt}\bar{\mu} = A\bar{\mu} + \sum_j(\sigma C_j + \Gamma_j)dW_j,
\tag{13a}
$$

$$
\frac{d}{dt}\sigma = A\sigma + \sigma A^T + D - \sum_j(\sigma C_j + \Gamma_j)(\sigma C_j + \Gamma_j)^T,
\tag{13b}
$$

where

$$
A = \begin{pmatrix}
-\frac{\kappa_c}{2} & \Delta_c & -\frac{G_c}{2} & 0 \\
\Delta_c & -\frac{\kappa_c}{2} & 2G_\omega + \frac{G_\kappa\Delta_c}{\kappa_c} & 0 \\
0 & 0 & -\frac{\gamma_m}{2} & \omega_m \\
2G_\omega + \frac{G_\kappa\Delta_c}{\kappa_c} & -\frac{G_c}{2} & -\omega_m & -\frac{\gamma_m}{2}
\end{pmatrix},
$$

$$
D = \begin{pmatrix}
\frac{\kappa_c}{2} & 0 & 0 & 0 \\
0 & \frac{\kappa_c}{2} & 0 & \frac{G_\kappa}{2} \\
0 & 0 & \tilde{\gamma}_m & 0 \\
0 & \frac{G_\kappa}{2} & 0 & \tilde{\gamma}_m + \frac{G_\kappa^2}{2\kappa_c} + \Gamma_m
\end{pmatrix},
$$

$$
C_1^T = \sqrt{2\eta_c\kappa_c}\left(\cos\phi_c, -\sin\phi_c, \frac{G_\kappa}{\kappa_c}\cos\phi_c, 0\right),
$$

$$
\Gamma_1^T = \sqrt{\frac{\eta_c\kappa_c}{2}}\left(-\cos\phi_c, \sin\phi_c, 0, \frac{G_\kappa}{\kappa_c}\sin\phi_c\right),
$$

$$
C_2^T = 2\sqrt{\eta_t\Gamma_m}(0, 0, 1, 0),
$$

$\Gamma_2 = 0$, and $\tilde{\gamma}_m = \gamma_m(\bar{n}_{th}+\frac{1}{2})$. In the above, C_j and Γ_j are determined, respectively, by the detection outcomes and the correlations between the input noises of the system and the detection noises. When the detection efficiencies $\eta_j = 1$, perfect correlations between the two noises are generated and optimal detection is achieved. It can be seen that Eq. (13a) for

the first moments is stochastic and dependent on the results of the time-continuous measurements, while the equation for the correlation matrix is deterministic and independent of the measurement results. The stochastic first-order moments can be removed by introducing a linear Markovian feedback to drive the system. The time-continuous measurements not only modify the drift and diffusion matrices of the system, but also induce nonlinear terms embodied by the terms $\sum_j \sigma C_j C_j^T \sigma$. In the absence of the measurements $\eta_j = 0$, Eq. (13a) for the first-order terms disappears and the nonlinear equation of Eq. (13b) reduces to the linear one with drift and diffusion matrices A and D.

D. Stability

When interested in the regime of steady states, we can set the time deviation equal to zero. In the absence of the continuous measurements, the linear equation is stable when the real parts of all eigenvalues of the matrix A are negative. It can be found that without the transducer field, the stable condition for the linearized optomechanical system with dissipative or dispersive coupling is that the following three inequalities are simultaneously held:

$$S_1 = \kappa_c\left(\frac{\kappa_c^2}{4} + \kappa_c\gamma_m + \Delta_c^2\right) + \gamma_m\left(\frac{\gamma_m^2}{4} + \kappa_c\gamma_m + \omega_m^2\right)$$
$$- 2\omega_m G_\kappa G > 0, \quad (14a)$$

$$S_2 = \left(\frac{\gamma_m^2}{4} + \omega_m^2\right)\left(\frac{\kappa_c^2}{4} + \Delta_c^2\right) + \kappa_c\omega_m G_\kappa G$$
$$+ 2\omega_m\Delta_c\left(\frac{G_\kappa^2}{8} - 2G^2\right) > 0, \quad (14b)$$

$$S_3 = \left[\kappa_c\left(\frac{\kappa_c\gamma_m}{4} + \omega_m^2\right) + \gamma_m\left(\frac{\kappa_c\gamma_m}{4} + \Delta_c^2\right) + 2\omega_m G_\kappa G\right]$$
$$\times \left[\kappa_c\left(\frac{\kappa_c^2}{4} + \kappa_c\gamma_m + \Delta_c^2\right) + \gamma_m\left(\frac{\gamma_m^2}{4} + \kappa_c\gamma_m + \omega_m^2\right)\right.$$
$$\left. - 2\omega_m G_\kappa G\right] - (\kappa_c + \gamma_m)^2\left[\left(\frac{\gamma_m^2}{4} + \omega_m^2\right)\left(\frac{\kappa_c^2}{4} + \Delta_c^2\right)\right.$$
$$\left. + \kappa_c\omega_m G_\kappa G + 2\omega_m\Delta_c\left(\frac{G_\kappa^2}{8} - 2G^2\right)\right] > 0, \quad (14c)$$

where $G = G_\omega + \frac{\Delta_c}{2\kappa_c}G_\kappa$. In the presence of the measurements, Eq. (13b) is stable when [72]

$$Cx_\lambda \neq 0 \; \forall x_\lambda : \tilde{A}x_\lambda = \lambda x_\lambda \text{ with } \mathrm{Re}(\lambda) \geqslant 0, \quad (15)$$

where $C = C_1^T + C_2^T$ and $\tilde{A} = A - (\Gamma_1 C_1^T + \Gamma_2 C_2^T)$.

III. NUMERICAL RESULTS

In this section, we investigate in detail the properties of the mechanical squeezing and optomechanical entanglement and steering in the optomechanical system under the time-continuous measurements. The mechanical squeezing can be measured by the variance of the generalized quadrature $\hat{X}_m^{\phi_m} \equiv \frac{1}{\sqrt{2}}(\hat{b}_m e^{i\phi_m} + \hat{b}_m^\dagger e^{-i\phi_m})$,
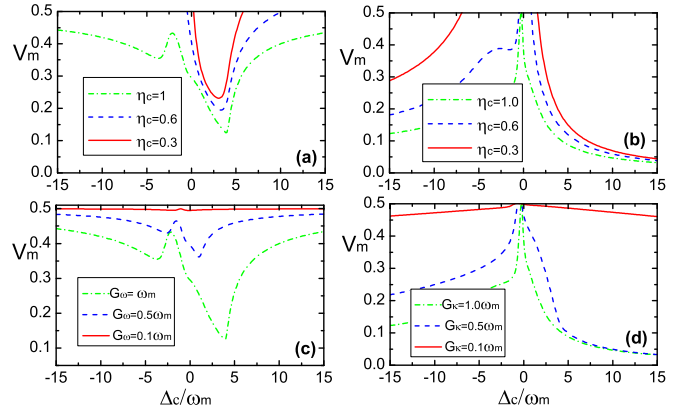
$$V_m^{\phi_m} = \langle(\hat{X}_m^{\phi_m})^2\rangle. \quad (16)$$

FIG. 2. The dependence of the mechanical squeezing V_m on the detuning Δ_c for (a),(c) purely dispersive coupling and for (b),(d) purely dissipative coupling. (a),(b) The coupling $G_\omega = \omega_m$ and $G_\kappa = \omega_m$; (c),(d) the detection efficiency $\eta_c = 1.0$. The other parameters $\kappa_c = \omega_m$, $\gamma_m = 10^{-5}\omega_m$, and $\bar{n}_{th} = 0$.

The squeezing is achieved when $V_m < \frac{1}{2}$. The optimal squeezing, with respect to the local angle ϕ_m, is equal to the minimal eigenvalues of the correlation matrix σ_m of the mechanical oscillator, i.e.,

$$V_m = \mathrm{Min}\{\mathrm{Eigen}[\sigma_m]\}, \quad (17)$$

when expressing the covariance matrix σ in the form

$$\sigma = \begin{pmatrix} \sigma_c & C_{cm} \\ C_{cm}^T & \sigma_m \end{pmatrix}. \quad (18)$$

Similarly, the optimal squeezing of the cavity field is $V_c = \mathrm{Min}\{\mathrm{Eigenvalues}[\sigma_c]\}$.

The steering from the cavity field $\hat{a}_c$ to the mechanical oscillator $\hat{b}_m$ can be quantified by the measure [73]

$$\mathcal{S}_{m|c} = \max\left\{0, \frac{1}{2}\ln\frac{\det\sigma_c}{4\det\sigma}\right\}. \quad (19)$$

Similarly, for the reverse steering from the mechanical oscillator to the cavity field, it is quantified by

$$\mathcal{S}_{c|m} = \max\left\{0, \frac{1}{2}\ln\frac{\det\sigma_m}{4\det\sigma}\right\}. \quad (20)$$

In addition, the entanglement between the cavity field $\hat{a}_c$ and the mechanical oscillator $\hat{b}_m$ can be quantified by the logarithmic negativity [74],

$$\mathcal{E}_{mc} = \max[0, -\ln(2e)], \quad (21)$$

where $e = 2^{-1/2}\sqrt{\Sigma^2(\sigma) - \sqrt{\Sigma^2(\sigma) - 4\det\sigma}}$ and $\Sigma(\sigma) = \det\sigma_c + \det\sigma_m - 2\det C_{cm}$.

A. Mechanical squeezing

We first study the mechanical squeezing by numerically solving the Riccati equation for Eq. (13b) in the steady-state regime with the software MATHEMATICA. In our numerical calculation, the local angles ϕ_c are chosen such that the mechanical squeezing is optimized (similarly hereinafter). In addition, we also set $\Gamma_m = 0$ in this section. In Fig. 2, the
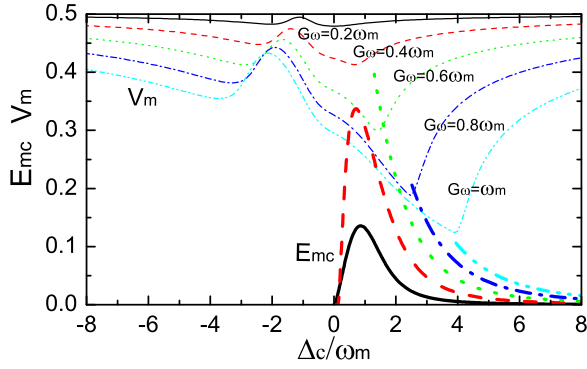
FIG. 3. The dependence of the mechanical squeezing V_m (thin curves) on the detuning Δ_c for purely dispersive coupling for different coupling strengths G_ω. The other parameters $\gamma_m = 10^{-5}\omega_m$, $\bar{n}_{th} = 0$, and $\eta_c = 1.0$. The thick curves depict the corresponding entanglement E_{mc} between the intracavity field and the mechanical oscillator in the absence of the detection ($\eta_c = 0$).

dependence the mechanical variance V_m on the output of the cavity field $\hat{a}_c$ on the detuning Δ_c is plotted. We note that in the absence of the detection $\eta_c = 0$, the variance $V_m > \frac{1}{2}$. But we can see from Fig. 2 that with the measurement, the mechanical squeezing beyond the 3 dB limit (i.e., $V_m < 1/4$) can be achieved not only by purely dispersive but also by purely dissipative coupling. This is because the optomechanical correlations are established via the dispersive or dissipative coupling and the homodyne detection on the output of the cavity field can therefore decrease the quadrature fluctuations of the mechanical subsystem. It is shown that the squeezing is dependent on the detection efficiency η_c. For the case of purely dispersive coupling, as the coupling strength G_ω decreases, the maximal squeezing decreases and it moves further away, approximately from $\Delta_c \approx 3.5\omega_m$ to $\Delta_c \approx 0$, as similarly obtained in Ref. [63] for a levitating nonsphere. For a fixed coupling strength, the squeezing degree decreases as the detuning $|\Delta_c|$ increases. This is because, as the detuning arises, the effective coupling between the cavity field and the mechanical oscillator is weakened, which in turn decreases the correlations between the two subsystems. Therefore, the mechanical squeezing is reduced. This can also be affirmed from Fig. 3, which plots the mechanical squeezing and the entanglement between the intracavity field and the mechanical oscillator. It is shown that the maximal squeezing occurs at the detuning at which the light-mechanical entanglement is maximum in the absence of the detection. As shown in Figs. 2(b) and 2(d), the behavior of the mechanical squeezing via purely dissipative coupling is quite different from that by purely dispersive coupling. We see that the squeezing disappears for the near-resonant coupling ($\Delta_c \approx 0$). As the detuning increases, the degree of squeezing is enhanced. This is because when the coupling G_ω or G_κ is fixed, the amplitude $\bar{a}_c^{ss}$ of the intracavity field $\hat{a}_c$ should be unchanged ($G_\omega = g_{c\omega}\bar{a}_c^{ss}$, $G_\kappa = g_{c\kappa}\bar{a}_c^{ss}$), which thus requires the power of the driving laser to be increased when the detuning increases. This means the classical amplitude $\bar{a}_s^{in}$ of the input field $\hat{a}_c^{in}$, which is directly coupled to the motion $\hat{X}_m$ of the mechanical oscillator, correspondingly increases for purely dissipative coupling. Therefore, the increasing of
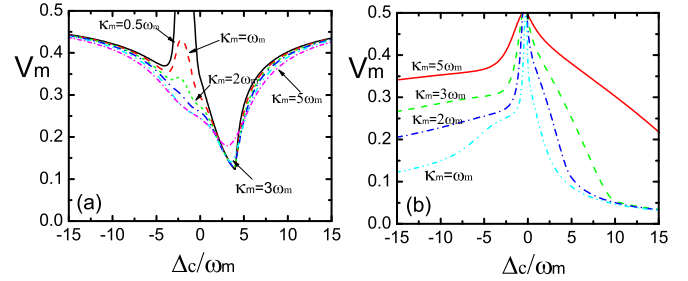

FIG. 4. The dependence of the mechanical squeezing V_m on the detuning Δ_c for purely dispersive coupling in (a) with $G_\omega = \omega_m$ and for purely dissipative coupling in (b) with $G_\kappa = \omega_m$, for different cavity dissipation rates κ_c. The other parameters $\gamma_m = 10^{-5}\omega_m$, $\bar{n}_{th} = 0$, and $\eta_c = 1.0$.

the detuning implies the increase of the effective dissipative optomechanical coupling, although the coupling G_κ is fixed. This is clearly embodied by the effective Hamiltonian in Eq. (5), where the term related to $\frac{G_\kappa\Delta_c}{\kappa_c}$ shows that the increase of the detuning leads to the enhancement of the coupling between the cavity field and the mechanical oscillator. As a consequence, the mechanical squeezing via the detection increases at first and then gets saturated as the detuning increases. In addition, we can also see that the mechanical squeezing vanishes at the approximate resonance $\Delta_c \approx 0$, since we have $\frac{G_\kappa\Delta_c}{\kappa_c} \approx 0$, although the coupling $G_\kappa \neq 0$ and the dissipative optomechanical coupling (the terms related to G_κ in the third and last lines) exist. This implies that the optomechanical correlations which determine the optimal mechanical squeezing via detection are mainly attributed to the effective coherent optomechanical coupling in Eq. (5).

In Fig. 4, the dependence of the mechanical squeezing on the detuning Δ_c for different values of the cavity dissipation rate κ_c is plotted. For the case of purely dispersive coupling, the increase of κ_c means the increase of the detection strength. Thus we see that the squeezing is improved around the detuning $\Delta_c \approx -2.5\omega_m$ and for $\Delta_c \gg 3.5\omega_m$, whereas for the purely dissipative coupling, the increase of κ_c brings about the improvement of the squeezing. Also, this is mainly because, as shown from Eq. (5) and discussed above, the coupling strength $\frac{G_\kappa\Delta_c}{\kappa_c}$ increases with the decreasing of κ_c. Physically, as explained above, for fixed coupling G_κ and driving power, the decreasing of κ_c leads to the increase of $\bar{a}_c^{in}$ and thus the increase of the dissipative coupling.

In Fig. 5, we consider the generation of the mechanical squeezing by the detection in the simultaneous presence of dispersive and dissipative coupling. In fact, recent experiments have already achieved the simultaneous occurrence of the two types of coupling [75–77]. We see that the combination of the two types of coupling leads the mechanical squeezing to be considerably enhanced, even with weaker coupling strengths, compared to the case of purely dispersive or purely dissipative coupling. For instance, with the coupling $G_\kappa = \frac{1}{2}G_\omega = \frac{1}{4}\omega_m$, the optimal variance $V_m \approx 0.1$ with the detuning $\Delta_c = 5\omega_m$. This allows us to produce strong mechanical squeezing merely by utilizing weak optomechanical coupling. In addition, we see that the enhancement occurs just for $\Delta_c > 0$, which is because, as shown in Eq. (5), the
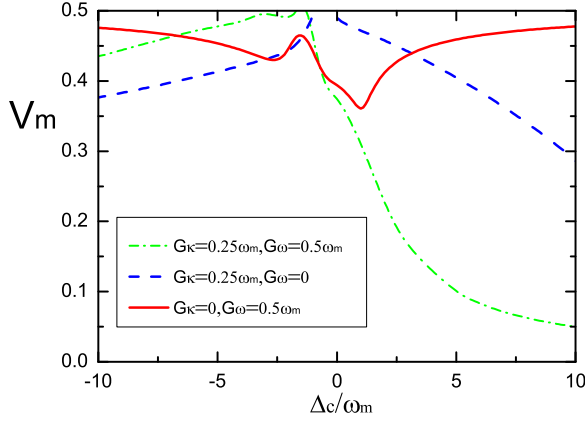
FIG. 5. The dependence of the mechanical squeezing V_m on the detuning Δ_c for purely dispersive coupling (solid line), for purely dissipative coupling (dashed line), and for the combination of the two types of couplings (dash-dotted line). The other parameters $\kappa_c = \omega_m$, $\gamma_m = 10^{-5}\omega_m$, $\bar{n}_{th} = 0$, and $\eta_c = 1.0$.

coupling strength $G_\omega + \frac{G_\kappa \Delta_c}{\kappa_c}$ is reduced for $\Delta_c < 0$, whereas it is enhanced for $\Delta_c > 0$.

So far, we have investigated the mechanical squeezing via homodyne detection under the vacuum environment of the mechanical oscillator. We now investigate the effect of the thermal environment on the mechanical squeezing, with realistic parameters close to recent relevant experiments. For purely dispersive coupling [78,79], we consider the mechanical frequency $\omega_m/2\pi \approx 5$ MHz, the cavity dissipation rate $\kappa_c/2\pi \approx 10$ MHz, the mechanical quality factor $Q_m = \frac{\omega_m}{\gamma_m} \approx 10^5$, and the single-photon coupling strength $g_{c\omega}/2\pi \approx 90$ Hz. When choosing the detuning $\Delta_c \approx 3.7\omega_m$, we have the collective dispersive coupling $G_\omega/2\pi \approx 5$ MHz for the power of pumping laser $\mathcal{P} \approx 150~\mu$W with pumping frequency $\nu_p/2\pi \approx 5$ GHz in the microwave regime. As shown in Fig. 6,
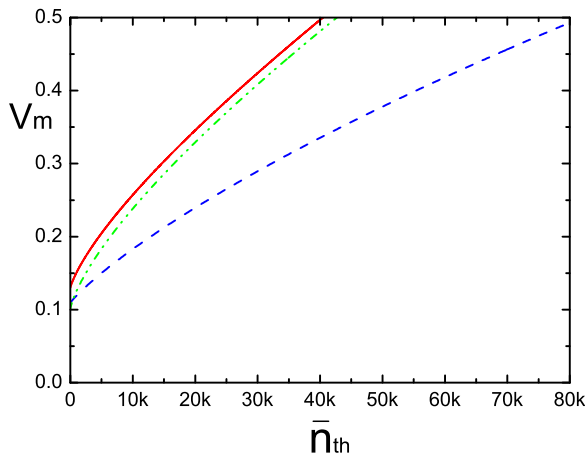

FIG. 6. The effect of thermal phonons on the mechanical squeezing V_m for purely dispersive coupling (solid line) with $G_\omega = \omega_m$, $\kappa_c = 2\omega_m$, and $\Delta_c = 3.7\omega_m$; for purely dissipative coupling (dashed line) with $G_\kappa = \omega_m$, $\kappa_c = 2\omega_m$, and $\Delta_c = 5\omega_m$; and for the combination of the coupling (dash-dot-dotted line) $G_\omega = 0.5\omega_m$, $G_\kappa = 0.25\omega_m$, $\kappa_c = \omega_m$, and $\Delta_c = 5\omega_m$. The other parameters $\gamma_m = 10^{-5}\omega_m$ and $\eta_c = 1.0$.
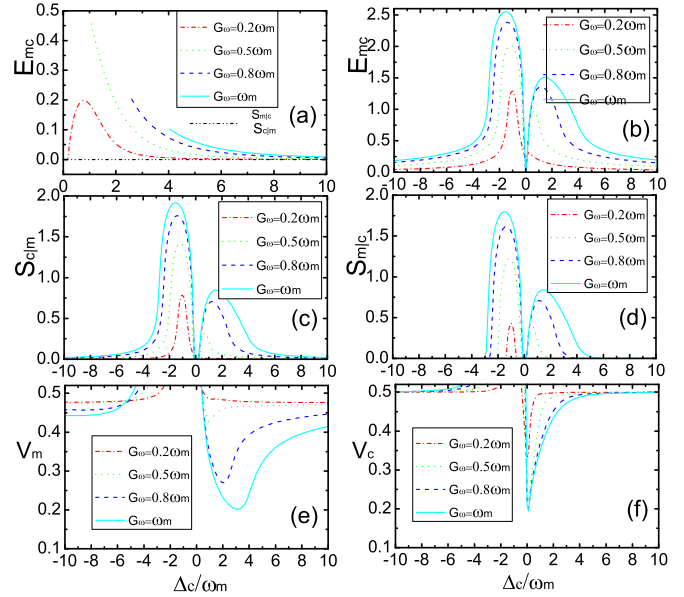

FIG. 7. The dependence of the optomechanical entanglement E_{mc}, the optomechanical steering $S_{c|m}$ and $S_{m|c}$, the mechanical squeezing V_m, and the cavity-field squeezing V_c on the detuning Δ_c via purely dispersive coupling G_ω. The other parameters $G_\kappa = 0$, $\kappa_c = 0.2\omega_m$, $\gamma_m = 10^{-5}\omega_m$, $\bar{n}_{th} = 0$, $\Gamma_m = 0.05\omega_m$, and $\eta_t = 1.0$. (a) The entanglement and steering in the absence of the detection ($\Gamma_m = 0$ and $\eta_t = 0$).

we see that the mechanical squeezing via purely dispersive coupling can exist up to the thermal phonon number $\bar{n}_{th} \approx 3.5 \times 10^4$, while for the case of purely dissipative coupling, we consider the parameters, proposed in Ref. [80] and realized in Ref. [75], as $\omega_m/2\pi \approx 130$ kHz, $\kappa_c/2\pi \approx 260$ kHz, $Q_m \approx 10^5$, and the single-photon coupling strength $g_{c\kappa}/2\pi \approx 2.5$ Hz. When the detuning $\Delta_c \approx 5\omega_m$, the coupling $G_\kappa \approx \omega_m$ for the pumping power $\mathcal{P} \approx 50$ mW with the wavelength $\lambda_p \approx 1064$ nm, and we have $\bar{n}_{th} \approx 4 \times 10^4$. Meanwhile, for the combination of the coupling, with the single-photon coupling $g_{c\omega} \approx 0.8$ Hz and $g_{c\kappa}/2\pi \approx 0.4$ Hz, the coupling $G_\omega = 2G_\kappa \approx 0.5\omega_m$ for the pumping power $\mathcal{P} \approx 400$ mW with the detuning $\Delta_c = 5\omega_m$, we have the maximal number of thermal phonons $\bar{n}_{th} \approx 8 \times 10^4$. These results show that the present scheme for generating mechanical squeezing is robust against thermal fluctuations.

B. Optomechanical steering

We proceed to discuss the optomechanical steering of the system under the continuous mechanical position monitoring. In Figs. 7 and 8, we plot the optomechanical entanglement, steering, and optical and mechanical squeezing, respectively, for purely dispersive and purely dissipative coupling. As shown in Fig. 7(a), without the continuous position monitoring, the entanglement via dispersive coupling is present only in the regime of red detuning $\Delta_c > 0$ and it maximizes approximately at $\Delta_c = \omega_m$ for weak coupling G_ω, which has already been studied in Ref. [81]. The optomechanical steering cannot be generated, while for dissipative coupling, the entanglement and steering are achievable in the blue-detuned regime when the monitoring is absent, as depicted in Fig. 8(a).
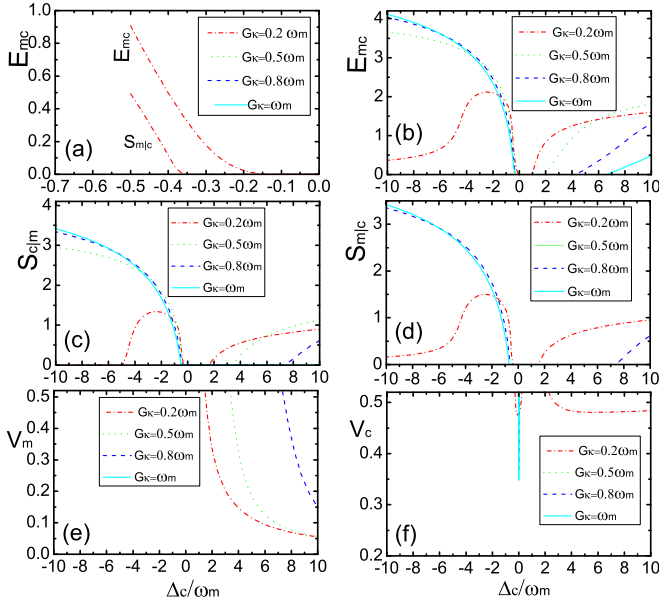
FIG. 8. The dependence of the optomechanical entanglement E_{mc}, the optomechanical steering $S_{c|m}$ and $S_{m|c}$, the mechanical squeezing V_m, and the cavity-field squeezing V_c on the detuning Δ_c via purely dissipative coupling G_κ. The other parameters $G_\omega = 0$, $\kappa_c = 0.2\omega_m$, $\gamma_m = 10^{-5}\omega_m$, $\bar{n}_{th} = 0$, $\Gamma_m = 0.05\omega_m$, and $\eta_t = 1.0$. (a) The situation without the detection ($\Gamma_m = 0$ and $\eta_t = 0$).
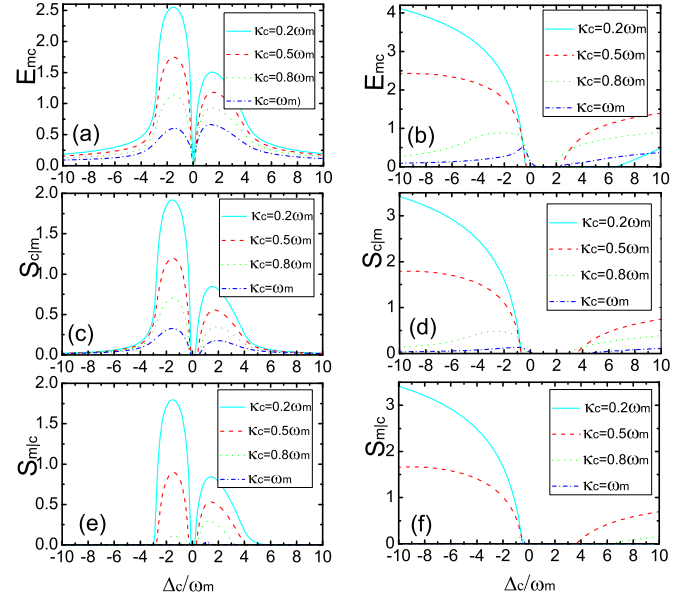

FIG. 9. The dependence of the optomechanical entanglement E_{mc} and the optomechanical steering $S_{c|m}$ and $S_{m|c}$ on the detuning Δ_c for (a),(c),(e) purely dispersive coupling $G_\omega = \omega_m$ and for (b),(d),(f) purely dissipative coupling $G_\kappa = \omega_m$, for different rates κ_c of cavity dissipation. The other parameters $\gamma_m = 10^{-5}\omega_m$, $\bar{n}_{th} = 0$, $\Gamma_m = 0.05\omega_m$, and $\eta_t = 1.0$.

However, when the monitoring is present, it can be seen that for both types of coupling, the entanglement is considerably enhanced such that strong optomechanical steering in both directions can be achieved. The entanglement and steering in the presence of the monitoring can be achieved in both regimes of red and blue detuning. In addition, it is shown in Figs. 7 and 8, with the position monitoring, the mechanical and optical squeezing can also be generated for two types of coupling. Physically, we can understand the above entanglement enhancement as follows: on one hand, the continuous monitoring extends the instability region to the blue-detuned regime which favors the generation of entanglement since the optomechanical parametric downconversion process [the terms $\hat{a}_c\hat{b}_m$ and $\hat{a}_c^\dagger\hat{b}_m^\dagger$ in Eq. (11)], which is responsible for the entanglement in this regime, is dominant. We therefore see that the entanglement and steering in the blue-detuned regime are stronger than that in the red-detuned regime for two kinds of coupling. On the other hand, the monitoring greatly reduces quantum fluctuations of the quadratures of the mechanical oscillator and the cavity field (e.g., squeezing generation), leading the entanglement to be enhanced, even in the regime of red detuning. It is shown in Fig. 7 that for dispersive coupling, the entanglement and steering maximize at $\Delta_c \approx -\omega_m$ in the blue-detuned regime. This is because, at this detuning, the resonant optomechanical parametric downconversion is achieved, while for dissipative coupling, as the detuning $-\Delta_c$ increases, the strength of the parametric downconversion coupling increases, and thus the maxima of the entanglement and steering do not occur at this detuning but at $|\Delta_c| \gg \omega_m$ for strong coupling.

In Fig. 9, the effect of the cavity dissipation rate κ_c on the entanglement and steering is plotted, respectively,

for purely dispersive and purely dissipative coupling. Obviously, the entanglement and steering decrease as κ_c increases due to the increased decoherence of the cavity field. Nevertheless, for the present system, the entanglement and steering can still be achieved even for $\kappa_c > \omega_m$. The field-to-oscillator steering decreases faster than the reverse steering and, further, we can see that one-way steering, e.g., $S_{m|c} = 0$ and $S_{m|c} \neq 0$, can be achieved. The asymmetric steering makes steerable correlations distinct from the entanglement. Essentially, this asymmetry results from the unequal damping rates of the cavity field and the mechanical oscillator. As the cavity dissipation increases, the fluctuations of the quadratures of the cavity field increase and the field is more difficult to steer by the mechanics. Therefore, here the asymmetric quantum correlations can be observed by adjusting the detuning with the chosen dissipation rate.

In Fig. 10, the effect of finite detection efficiency η_t is investigated with the cavity dissipation rate $\kappa_c < \omega_m$. It is shown that the entanglement and steering can be enhanced by increasing the detection efficiency. It can be easily found that in the regimes, where the optomechanical system is unstable without the monitoring, the short-time entanglement is almost equal to the steady-state entanglement with the monitoring in these regimes. This implies that the continuous weak measurement of the position of the mechanical oscillator merely alters the stability and the steady-state entanglement and steering in the presence of the measurement in these regimes is still mainly determined just by the system's parameters. Therefore, we see that the steady-state entanglement and steering around the peaks are sightly improved by increasing the detection efficiency.
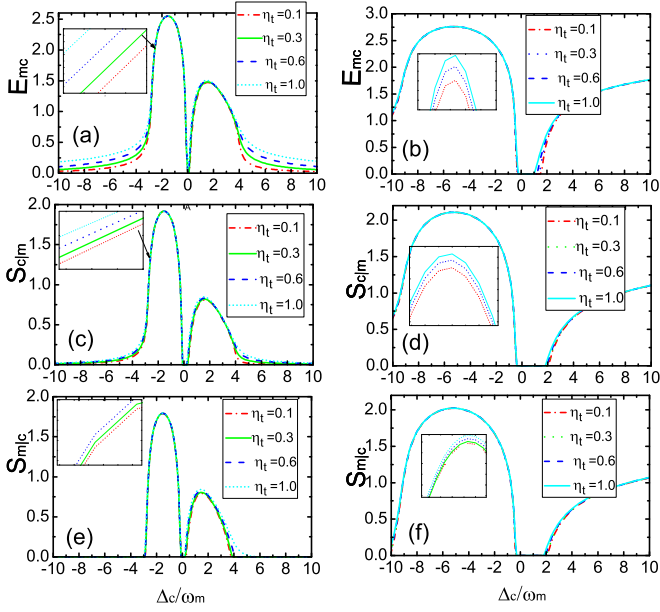
FIG. 10. The dependence of the optomechanical entanglement E_{mc} and optomechanical steering $S_{c|m}$ and $S_{m|c}$ on the detuning Δ_c for (a),(c),(e) purely dispersive coupling $G_\omega = \omega_m$ and for (b),(d),(f) purely dissipative coupling $G_\kappa = 0.3\omega_m$, for different values η_t of detection efficiency. The other parameters $\kappa_c = 0.2\omega_m$, $\gamma_m = 10^{-5}\omega_m$, $\bar{n}_{th} = 0$, and $\Gamma_m = 0.05\omega_m$.

In Fig. 11, the entanglement and steering are plotted for the combination of two kinds of coupling. We see that similar to the mechanical squeezing, the entanglement and steering are also enhanced in the regime of red detuning $\Delta_c > 0$ in which the effective strength of optomechanical coupling in Eq. (5) is increased, while in the regime of blue detuning $\Delta_c < 0$, the effective coupling strength is decreased and thus the entanglement and steering are reduced, compared to that via purely dissipative coupling.

Finally, we study the effect of the thermal environment on the entanglement and steering, which is plotted in Fig. 12. For purely dispersive coupling, we consider the parameters in the previous section, but with the cavity dissipation rate $\kappa_c/2\pi \approx 1$ MHz, the detuning $\Delta_c \approx -2\omega_m$, and the collective
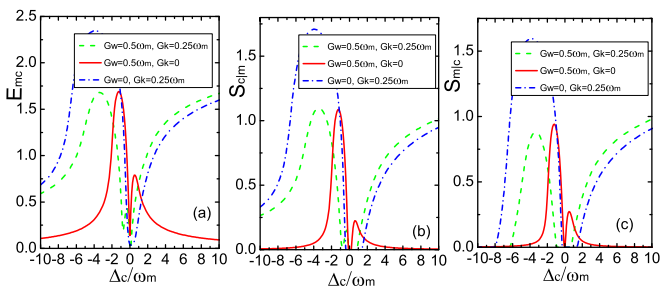

FIG. 11. The dependence of the (a) optomechanical entanglement E_{mc}, and the (b) optomechanical steering $S_{c|m}$ and (c) $S_{m|c}$ on the detuning Δ_c for purely dispersive coupling, for purely dissipative coupling, and for the combination of two types of coupling. The other parameters $\kappa_c = 0.2\omega_m$, $\gamma_m = 10^{-5}\omega_m$, $\bar{n}_{th} = 0$, $\Gamma_m = 0.05\omega_m$, and $\eta_t = 1.0$.
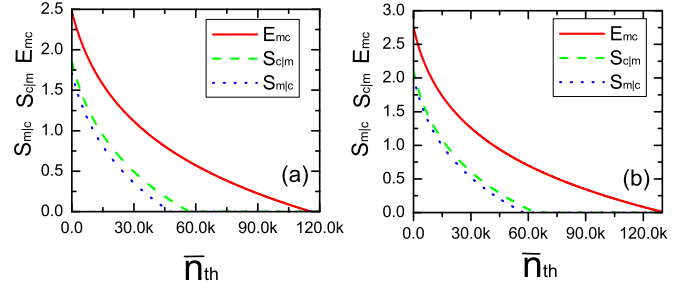

FIG. 12. The effect of thermal phonons on the optomechanical entanglement E_{mc}, and the optomechanical steering $S_{c|m}$ and $S_{m|c}$ for (a) purely dispersive coupling, with $G_\omega = \omega_m$ and $\Delta_c = -2\omega_m$, and for (b) purely dissipative coupling, with $G_\kappa = 0.3\omega_m$ and $\Delta_c = -5\omega_m$. The other parameters $\kappa_c = 0.2\omega_m$, $\gamma_m = 10^{-5}\omega_m$, $\Gamma_m = 0.05\omega_m$, and $\eta_t = 1.0$.

dispersive coupling $G_\omega/2\pi \approx 5$ MHz for the pump power $\mathcal{P} \approx 0.2$ μW. In addition, we can also consider a lower-frequency mechanical resonator, as in Ref. [71] in which the mechanically mediated indirect coupling between optical and microwave fields has been realized. For this system, we assume that the optical cavity plays the role of the transducer cavity and choose the mechanical frequency $\omega_m/2\pi = 400$ kHz and mechanical damping $\gamma_m/2\pi \approx 4$ Hz. For the dissipation rate of the optical cavity $\kappa_t/2\pi \approx 2$ MHz, the condition is that the damping rate $\Gamma_m = 0.05\omega_m$ requires the pumping power $\mathcal{P}_t \approx 25$ μW with the optical frequency $\omega_t/2\pi \approx 280$ THz and the single-photon coupling $g_t/2\pi \approx 7$ Hz. When choosing the loss rate of the microwave cavity $\kappa_c \approx 0.2\omega_m$ and the detuning $\Delta_c \approx -2\omega_m$, one can also achieve the coupling $G_c \approx \omega_m$, with the pumping power $\mathcal{P}_c \approx 10$ μW for the single-photon coupling $g_c/2\pi \approx 2$ Hz and the microwave frequency $\omega_c/2\pi \approx 7$ GHz. As shown in Fig. 12(a), the maximal thermal phonon numbers for achieving the entanglement and steering are, respectively, $\bar{n}_{th} \approx 1.15 \times 10^5$ and $\bar{n}_{th} \approx 5.6 \times 10^4$ ($S_{c|m}$), while for the case of purely dissipative coupling, we consider $\kappa_c/2\pi \approx 26$ kHz, the detuning $\Delta_c \approx -5\omega_m$, and the coupling $G_\kappa \approx \omega_m$ for the pumping power $\mathcal{P} \approx 180$ mW. The maximal thermal phonon numbers for generating the entanglement and steering are, respectively, $\bar{n}_{th} \approx 1.27 \times 10^5$ and $\bar{n}_{th} \approx 6.3 \times 10^4$. Therefore, the present scheme can be used for generating robust optomechanical steerable correlations by continuously monitoring the mechanical position.

IV. DISCUSSION AND CONCLUSION

Before concluding, we briefly discuss how to verify the generated mechanical squeezing and optomechanical steering. Similarly to the protocol proposed in Ref. [82], for the mechanical squeezing, we can couple the mechanical resonator to another weakly driven probe cavity which is resonant to the red sideband of the drive. The beam-splitter-like coupling is induced between the mechanical oscillator and the probe cavity field and the mechanical states can thus be mapped onto the probe cavity field. Then, by homodyning the output field of the probe cavity, one can detect the mechanical squeezing. For the verification of the optomechanical steering, we cannot use the transducer cavity as the probe cavity because it is a

bad cavity. In principle, one can also couple the mechanical resonator to a third cavity, but this will make the system too complicated. Thus, we employ a weak probe field sent into the cavity $\hat{a}_c$. Likewise, the probe field is tuned to be resonant to the lower sideband of the cavity field $\hat{a}_c$ to induce the beam-splitter-like interaction between the probe field and the mechanical oscillator. By keeping the frequency separate between the probe field and the cavity field $\hat{a}_c$ much larger than the linewidth κ_c^{-1}, we can resolve the two output fields of the probe and cavity fields. Then, by homodyning the output fields and combining them, we can verify the optomechanical steering.

In conclusion, in this paper we first consider the generation of mechanical squeezing in a dispersively or dissipatively coupled optomechanical system by continuously homodyning the output of the cavity field. It is found that strong steady-state mechanical squeezing can be achieved, but the properties of the squeezing are quite different for two types of coupling. In addition, the combination of the two types of coupling can also enhance the mechanical squeezing. We next consider the achievement of optomechanical steering in a dispersive or dissipative optomechanical system via continuously monitoring the position of the mechanical oscillator. The position monitoring can be realized by dispersively coupling the mechanical oscillator weakly to an overdamped transducer cavity whose output field is subject to continuous homodyne detection. It is revealed that the monitoring of the mechanical position can lead the steady-state optomechanical entanglement to be enhanced considerably such that strong optomechanical steerable correlations can be generated. In addition, the continuous monitoring can also bring about the simultaneous squeezing of the mechanical oscillator and cavity field. The effects of thermal phonons are also studied and it is shown that the generated squeezing and steering are robust against the thermal fluctuations.

APPENDIX: LANGEVIN EQUATION OF MOTION FOR THE MECHANICAL OSCILLATOR

In this Appendix, we will derive the Langevin equation of motion for a mechanical oscillator in a thermal bath. We consider that the mechanical mode $\hat{b}_m$ is coupled to a bath of harmonic oscillators, which is described by the Hamiltonian [83]

$$\hat{H}_{sb} = \omega_m \hat{b}_m^\dagger \hat{b}_m + \sum_k \omega_k \hat{d}_k^\dagger d_k + \sum_k g_k(\hat{b}_m + \hat{b}_m^\dagger)(\hat{d}_k^\dagger + \hat{a}_k),$$

(A1)

where the annihilation operator $\hat{b}_k$ denotes the kth oscillator of the bath with frequency ω_k and g_k represent the system-bath coupling. In the interaction picture, the above Hamiltonian becomes

$$\hat{H}_{sb} = \sum_k g_k \left[\hat{b}_m \hat{a}_k e^{-i(\omega_m + \omega_k)t} + \hat{b}_m \hat{a}_k^\dagger e^{-i(\omega_m - \omega_k)t} + \text{H.c.}\right].$$

(A2)

When the mechanical resonant frequency $\omega_m \gg g_k$ for the frequency ω_k in the vicinity of the resonance, the fast oscillating term $\hat{b}_m \hat{a}_k e^{-i(\omega_m + \omega_k)t}$ and its conjugate can be neglected. Then, the Hamiltonian can be approximated, in the original picture, into

$$\hat{H}_{sb} = \omega_m \hat{b}_m^\dagger \hat{b}_m + \sum_k \omega_k \hat{d}_k^\dagger d_k + \sum_k g_k(\hat{b}_m \hat{d}_k + \hat{b}_m \hat{d}_k^\dagger),$$

(A3)

which is the system-bath interaction that we have encountered in quantum optics textbooks [84,85]. With Eq. (A3), we obtain

$$\frac{d}{dt}\hat{b}_m = -i\omega_m \hat{b}_m - \sum_k g_k^2 \int_0^t dt' \hat{b}_m(t') e^{-i\omega_k(t-t')} - \hat{b}_{\text{in}}(t),$$

(A4)

where $\hat{b}_{\text{in}}(t) = i \sum_k g_k \hat{b}_k(0) e^{-i\omega_k t}$ is dependent only on the initial states of the bath oscillators. By replace $\hat{\tilde{b}}_m = \hat{b}_m e^{i\omega_m t}$ and $\sum_k \to \int d\omega$, we have [84,85]

$$\frac{d}{dt}\hat{\tilde{b}}_m = -\int_0^\infty d\omega g^2(\omega)\frac{dk}{d\omega}\int_0^t dt' \hat{\tilde{b}}_m(t') e^{-i(\omega - \omega_m)(t-t')} - \hat{\tilde{b}}_{\text{in}}(t),$$

$$\simeq -J(\omega_m)\int_0^t dt' \hat{\tilde{b}}_m(t')\int_{-\infty}^\infty d\omega e^{-i(\omega - \omega_m)(t-t')} - \hat{\tilde{b}}_{\text{in}}(t)$$

$$= -\frac{\gamma_m}{2}\hat{b}_m(t) - \hat{\tilde{b}}_{\text{in}}(t),$$

(A5)

where we have let $J(\omega) = g^2(\omega)\frac{dk}{d\omega}$, $J(\omega_m) = \frac{\gamma_m}{2\pi}$, and $\hat{\tilde{b}}_{\text{in}}(t) = i \sum_k g_k \hat{b}_k(0) e^{-i(\omega_k - \omega_m)t}$, which satisfies the correlation

$$\langle \hat{\tilde{b}}_{\text{in}}^\dagger(t)\hat{\tilde{b}}_{\text{in}}(t') \rangle = \int_0^\infty d\omega J(\omega)\bar{n}_{th}(\omega) e^{i(\omega_k - \omega_m)(t-t')}$$

$$\simeq \gamma_m \bar{n}_{th}(\omega_m)\delta(t - t'),$$

(A6)

when only the frequency components around the resonance ω_m contribute the above integrations. Equation (A5) describes the damping of the mechanical mode in the thermal bath, which is used in Eq. (4c).

[1] C. M. Caves, K. S. Thorne, R. W. P. Drever, V. D. Sandberg, and M. Zimmermann, Rev. Mod. Phys. **52**, 341 (1980).

[2] S. L. Braunstein and P. van Loock, Rev. Mod. Phys. **77**, 513 (2005).

[3] D. F. Walls and G. J. Milburn, *Quantum Optics* (Springer, New York, 2008).

[4] A. Nunnenkamp, K. Børkje, J. G. E. Harris, and S. M. Girvin, Phys. Rev. A **82**, 021806(R) (2010).

[5] K. Jähne, C. Genes, K. Hammerer, M. Wallquist, E. S. Polzik, and P. Zoller, Phys. Rev. A **79**, 063819 (2009).

[6] A. Szorkovszky, A. C. Doherty, G. I. Harris, and W. P. Bowen, Phys. Rev. Lett. **107**, 213603 (2011).

[7] G. S. Agarwal and S. M. Huang, Phys. Rev. A **93**, 043844 (2016).

[8] Xiang You, Zongyang Li, and Yongmin Li, Phys. Rev. A **96**, 063811 (2017).

[9] Xin-You Lü, Jie-Qiao Liao, Lin Tian, and Franco Nori, Phys. Rev. A **91**, 013834 (2015).

[10] A. Kronwald, F. Marquardt, and A. A. Clerk, Phys. Rev. A **88**, 063833 (2013).

[11] Chang-Sheng Hu, Zhen-Biao Yang, Huaizhi Wu, Yong Li, and Shi-Biao Zheng, Phys. Rev. A **98**, 023807 (2018).

[12] C. U. Lei, A. J. Weinstein, J. Suh, E. E. Wollman, A. Kronwald, F. Marquardt, A. A. Clerk, and K. C. Schwab, Phys. Rev. Lett. **117**, 100801 (2016).

[13] A. Einstein, B. Podolsky, and N. Rosen, Phys. Rev. **47**, 777 (1935).

[14] E. Schrödinger, Proc. Cambridge Philos. Soc. **31**, 555 (1935).

[15] J. S. Bell, Physics **1**, 195 (1964).

[16] N. Brunner, D. Cavalcanti, S. Pironio, V. Scarani, and S. Wehner, Rev. Mod. Phys. **86**, 419 (2014).

[17] H. M. Wiseman, S. J. Jones, and A. C. Doherty, Phys. Rev. Lett. **98**, 140402 (2007).

[18] S. J. Jones, H. M. Wiseman, and A. C. Doherty, Phys. Rev. A **76**, 052116 (2007).

[19] J. Bowles, T. Vértesi, M. T. Quintino, and N. Brunner, Phys. Rev. Lett. **112**, 200402 (2014).

[20] P. Skrzypczyk, M. Navascues, and D. Cavalcanti, Phys. Rev. Lett. **112**, 180404 (2014).

[21] V. Händchen, T. Eberle, S. Steinlechner, A. Samblowski, T. Franz, R. F. Werner, and R. Schnabel, Nat. Photon. **6**, 596 (2012).

[22] S. Wollmann, N. Walk, A. J. Bennet, H. M. Wiseman, and G. J. Pryde, Phys. Rev. Lett. **116**, 160403 (2016).

[23] K. Sun, X. J. Ye, J. S. Xu, X. Y. Xu, J. S. Tang, Y. C. Wu, J. L. Chen, C. F. Li, and G. C. Guo, Phys. Rev. Lett. **116**, 160404 (2016).

[24] Y. Xiao, X. J. Ye, K. Sun, J. S. Xu, C. F. Li, and G. C. Guo, Phys. Rev. Lett. **118**, 140404 (2017).

[25] C. Branciard, E. G. Cavalcanti, S. P. Walborn, V. Scarani, and H. M. Wiseman, Phys. Rev. A **85**, 010301(R) (2012).

[26] N. Walk, S. Hosseini, J. Geng, O. Thearle, J. Y. Haw, S. Armstrong, S. M. Assad, J. Janousek, T. C. Ralph, T. Symul, H. M. Wiseman, and P. K. Lam, Optica **3**, 634 (2016).

[27] M. Piani and J. Watrous, Phys. Rev. Lett. **114**, 060404 (2015).

[28] Q. He, L. Rosales-Zárate, G. Adesso, and M. D. Reid, Phys. Rev. Lett. **115**, 180502 (2015).

[29] Y. Shen, S. M. Assad, N. B. Grosse, X. Y. Li, M. D. Reid, and P. K. Lam, Phys. Rev. Lett. **114**, 100403 (2015).

[30] Y. Ma, H. Miao, B. H. Pang, M. Evans, Chunnong Zhao, J. Harms, R. Schnabel, and Yanbei Chen, Nat. Phys. **13**, 776 (2017).

[31] A. Mallick and S. Ghosh, Phys. Rev. A **96**, 052323 (2017).

[32] Q. Y. He and M. D. Reid, Phys. Rev. A **88**, 052121 (2013).

[33] D. J. Saunders, S. J. Jones, H. M. Wiseman, and G. J. Pryde, Nat. Phys. **6**, 845 (2010).

[34] K. Sun, J. S. Xu, X. J. Ye, Y. C. Wu, J. L. Chen, C. F. Li, and G. C. Guo, Phys. Rev. Lett. **113**, 140402 (2014).

[35] D. Cavalcanti, P. Skrzypczyk, G. H. Aguilar, R. V. Nery, P. H. Souto Ribeiro, and S. P. Walborn, Nat. Commun. **6**, 7941 (2015).

[36] S. Armstrong, M. Wang, R. Y. Teh, Q. Gong, Q. He, J. Janousek, H.-A. Bachor, M. D. Reid, and P. K. Lam, Nat. Phys. **11**, 167 (2015).

[37] S. Kocsis, M. J. W. Hall, A. J. Bennet, D. J. Saunders, and G. J. Pryde, Nat. Commun. **6**, 5886 (2015).

[38] T. Guerreiro, F. Monteiro, A. Martin, J. B. Brask, T. Vertesi, B. Korzh, M. Caloz, F. Bussieres, V. B. Verma, A. E. Lita, R. P. Mirin, S. W. Nam, F. Marsilli, M. D. Shaw, N. Gisin, N. Brunner, H. Zbinden, and R. T. Thew, Phys. Rev. Lett. **117**, 070404 (2016).

[39] X. Deng, Y. Xiang, C. Tian, G. Adesso, Q. He, Q. Gong, X. Su, C. Xie, and K. Peng, Phys. Rev. Lett. **118**, 230501 (2017).

[40] S. P. Walborn, A. Salles, R. M. Gomes, F. Toscano, and P. H. Souto Ribeiro, Phys. Rev. Lett. **106**, 130402 (2011).

[41] P. Meystre, Ann. Phys. **525**, 215 (2013); Y. Chen, J. Phys. B: At. Mol. Opt. Phys. **46**, 104001 (2013); M. Aspelmeyer, T. J. Kippenberg, and F. Marquardt, Rev. Mod. Phys. **86**, 1391 (2014).

[42] K. Stannigel, P. Rabl, A. S. Sørensen, P. Zoller, and M. D. Lukin, Phys. Rev. Lett. **105**, 220501 (2010).

[43] S. G. Hofer, W. Wieczorek, M. Aspelmeyer, and K. Hammerer, Phys. Rev. A **84**, 052327 (2011).

[44] V. Fiore, Y. Yang, M. C. Kuzyk, R. Barbour, L. Tian, and H. Wang, Phys. Rev. Lett. **107**, 133601 (2011).

[45] S. Rips and M. J. Hartmann, Phys. Rev. Lett. **110**, 120503 (2013).

[46] B. Vermersch, P.-O. Guimond, H. Pichler, and P. Zoller, Phys. Rev. Lett. **118**, 133601 (2017).

[47] The LIGO Scientific Collaboration, Nat. Phys. **7**, 962 (2011); H. Miao, Y. Ma, C. Zhao, and Y. Chen, Phys. Rev. Lett. **115**, 211104 (2015).

[48] S. Forstner, S. Prams, J. Knittel, E. D. van Ooijen, J. D. Swaim, G. I. Harris, A. Szorkovszky, W. P. Bowen, and H. Rubinsztein-Dunlop, Phys. Rev. Lett. **108**, 120801 (2012).

[49] G. I. Harris, D. L. McAuslan, T. M. Stace, A. C. Doherty, and W. P. Bowen, Phys. Rev. Lett. **111**, 103603 (2013).

[50] A. H. Safavi-Naeini, S. Gröblacher, J. T. Hill, J. Chan, M. Aspelmeyer, and O. Painter, Nature (London) **500**, 185 (2013).

[51] J. M. Pirkkalainen, E. Damskägg, M. Brandt, F. Massel, and M. A. Sillanpää, Phys. Rev. Lett. **115**, 243601 (2015).

[52] E. E. Wollman, C. U. Lei, A. J. Weinstein, J. Suh, A. Kronwald, F. Marquardt, A. A. Clerk, and K. C. Schwab, Science **349**, 952 (2015).

[53] T. A. Palomaki, J. D. Teufel, R. W. Simmonds, and K. W. Lehnert, Science **342**, 710 (2013).

[54] M. Ho, E. Oudot, J. D. Bancal, and N. Sangouard, Phys. Rev. Lett. **121**, 023602 (2018).

[55] C. F. Ockeloen-Korppi, E. Damskagg, J.-M. Pirkkalainen, A. A. Clerk, F. Massel, M. J. Woolley, and M. A. Sillanpaa, Nature (London) **556**, 478 (2018).

[56] R. Riedinger, S. Hong, R. A. Norte, J. A. Slater, J. Shang, A. G. Krause, V. Anant, M. Aspelmeyer, and S. Gröblacher, Nature (London) **530**, 313 (2016).

[57] S. Hong, R. Riedinger, I. Marinkovic, A. Wallucks, S. G. Hofer, R. A. Norte, M. Aspelmeyer, and S. Gröblacher, Science **358**, 203 (2017).

[58] I. Marinkovic, A. Wallucks, R. Riedinger, S. Hong, M. Aspelmeyer, and S. Gröblacher, Phys. Rev. Lett. **121**, 220404 (2018).

[59] S. G. Hofer, K. W. Lehnert, and K. Hammerer, Phys. Rev. Lett. **116**, 070406 (2016).

[60] A. Szorkovszky, G. A. Brawley, A. C. Doherty, and W. P. Bowen, Phys. Rev. Lett. **110**, 184301 (2013).

[61] W. Wieczorek, S. G. Hofer, J. H. Obermaier, R. Riedinger, K. Hammerer, and M. Aspelmeyer, Phys. Rev. Lett. **114**, 223601 (2015).

[62] S. G. Hofer and K. Hammerer, Phys. Rev. A **91**, 033822 (2015).

[63] M. G. Genoni, J. Zhang, J. Millen, P. F. Barker, and A. Serafini, New J. Phys. **17**, 073019 (2015).

[64] C. Schäfermeier, H. Kerdoncuff, U. B. Hoff, H. Fu, A. Huck, J. Bilek, G. I. Harris, W. P. Bowen, T. Gehring, and U. L. Andersen, Nat. Commun. **7**, 13628 (2016).

[65] M. Rossi, N. Kralj, S. Zippilli, R. Natali, A. Borrielli, G. Pandraud, E. Serra, G. Di Giuseppe, and D. Vitali, Phys. Rev. Lett. **119**, 123603 (2017).

[66] M. R. Vanner, I. Pikovski, G. D. Cole, M. S. Kim, C. Brukner, K. Hammerer, G. J. Milburn, and M. Aspelmeyer, Proc. Natl. Acad. Sci. **108**, 16182 (2011).

[67] M. R. Vanner, J. Hofer, G. D. Cole, and M. Aspelmeyer, Nat. Commun. **4**, 2295 (2013).

[68] G. A. Brawley, M. R. Vanner, P. E. Larsen, S. Schmid, A. Boisen, and W. P. Bowen, Nat. Commun. **7**, 10988 (2015).

[69] S. Barzanjeh, E. S. Redchenko, M. Peruzzo, M. Wulf, D. P. Lewis, G. Arnold, and J. M. Fink, Nature **570**, 480 (2019).

[70] L. Mercier de Lépinay, E. Damskägg, C. F. Ockeloen-Korppi, and M. A. Sillanpää, Phys. Rev. Appl. **11**, 034027 (2019).

[71] R. W. Andrews, R. W. Peterson, T. P. Purdy, K. Cicak, R. W. Simmonds, C. A. Regal, and K. W. Lehnert, Nat. Phys. **10**, 321 (2014).

[72] H. M. Wiseman and G. J. Milburn, *Quantum Measurement and Control* (Cambridge University Press, Cambridge, 2010).

[73] I. Kogias, A. R. Lee, S. Ragy, and G. Adesso, Phys. Rev. Lett. **114**, 060403 (2015).

[74] M. B. Plenio, Phys. Rev. Lett. **95**, 090503 (2005).

[75] A. Sawadsky, H. Kaufer, R. M. Nia, S. P. Tarabrin, F. Y. Khalili, K. Hammerer, and R. Schnabel, Phys. Rev. Lett. **114**, 043601 (2015).

[76] M. Wu, A. C. Hryciw, C. Healey, D. P. Lake, H. Jayakumar, M. R. Freeman, J. P. Davis, and P. E. Barclay, Phys. Rev. X **4**, 021052 (2014).

[77] B. Khanaliloo, H. Jayakumar, A. C. Hryciw, D. P. Lake, H. Kaviani, and P. E. Barclay, Phys. Rev. X **5**, 041051 (2015).

[78] N. R. Bernier, L. D. Tóth, A. Koottandavida, M. A. Ioannou, D. Malz, A. Nunnenkamp, A. K. Feofanov, and T. J. Kippenberg, Nat. Commun. **8**, 604 (2017).

[79] V. Sudhir, R. Schilling, S. A. Fedorov, H. Schütz, D. J. Wilson, and T. J. Kippenberg, Phys. Rev. X **7**, 031055 (2017).

[80] A. Xuereb, R. Schnabel, and K. Hammerer, Phys. Rev. Lett. **107**, 213604 (2011).

[81] C. Genes, A. Mari, P. Tombesi, and D. Vitali, Phys. Rev. A **78**, 032316 (2008).

[82] D. Vitali, S. Gigan, A. Ferreira, H. R. Böhm, P. Tombesi, A. Guerreiro, V. Vedral, A. Zeilinger, and M. Aspelmeyer, Phys. Rev. Lett. **98**, 030405 (2007).

[83] C. W. Gardiner and P. Zoller, *Quantum Noise* (Springer, Berlin, 2000), Chap. 3.

[84] D. F. Walls and G. J. Milburn, *Quantum Optics* (Springer, Berlin, 2008).

[85] M. O. Scully and M. S. Zubairy, *Quantum Optics* (Cambridge University Press, Cambridge, 2012).